

SERENDIPITOUS DISCOVERY OF A CANDIDATE DEBRIS DISK AROUND THE DA WHITE DWARF SDSS J114404.74+052951.6

JINCHENG GUO^{1,2}, ANESTIS TZIAMTZIS³, ZHONGXIANG WANG³, JIFENG LIU¹, JINGKUN ZHAO¹, AND SONG WANG¹

¹ Key Laboratory of Optical Astronomy, National Astronomical Observatories, Chinese Academy of Sciences, Beijing 100012, China; jcguo@nao.cas.cn

² University of Chinese Academy of Sciences, Beijing 100049, China

³ Shanghai Astronomical Observatory, Chinese Academy of Sciences, 80 Nandan Road, Shanghai 200030, China

Received 2015 June 29; accepted 2015 August 18; published 2015 September 2

ABSTRACT

We report our serendipitous discovery of a candidate debris disk around the recently identified DA white dwarf (WD) SDSS J114404.74+052951.6. The Ca II infrared (IR) triplet, while weakly detected in the source’s optical spectrum, shows a double-peak like profile, and near-IR excesses are also detected from broadband imaging. The two features are commonly seen in the WD gaseous debris disks, and thus indicate the existence of such a disk around the DA WD. We further analyze the emission lines and broadband IR excesses and estimate that the debris disk may have a size of 20–50 R_{WD} and an inclination angle of 82° . The estimated temperature and cooling age for this WD are 23,027 K and ~ 21 Myr, respectively, making it possibly one of the hottest and youngest among candidates of WD debris-disk systems. These properties are also in line with the likely conditions for having a sufficiently bright debris disk. Further observations of the source are warranted in order to determine the debris disk’s properties and search for more absorption features of heavy elements.

Key words: circumstellar matter – stars: individual (SDSS J114404.74+052951.6) – white dwarfs

1. INTRODUCTION

Since the first discovery of a debris disk around a white dwarf (WD; Zuckerman & Becklin 1987), 35 such disks have been confirmed to exist around their host WDs (Rocchetto et al. 2015). Seven of them have been found to contain gas, which are SDSS 1228+1040 (Gänsicke et al. 2006), SDSS 1043+0856 (Gänsicke et al. 2007), SDSS 0845+2257 (Gänsicke et al. 2008), HE 1349–2305 (Melis et al. 2012a), SDSS 0959–0200 (Farihi et al. 2012), SDSS 0738+1835, and SDSS 1617+1620 (Brinkworth et al. 2012). It is widely accepted that such a disk originates from the tidal disruption of asteroids, comets, or even planets within the Roche radius of a WD (Graham et al. 1990). These planetary objects are known to commonly exist around the progenitors of WDs and are regarded to be able to survive through the late phases of stellar evolution (Debes & Sigurdsson 2002; Veras et al. 2013).

Over the past decade, this scenario has been supported by observational results. Absorption features of high-Z metals are seen in the spectra of the so-called polluted WDs, indicating accretion as a common process for WDs (Zuckerman et al. 2003; Jura 2008; Klein et al. 2011). The debris disks, although comparably rare, are the natural structure for the accretion process. These in turn make studies of metal-polluted WDs of great interest since they can provide crucial information on the bulk elemental compositions of extrasolar planets (e.g., Zuckerman et al. 2007; Farihi et al. 2013; Xu et al. 2014; Raddi et al. 2015).

In this Letter, we report our serendipitous discovery of a candidate debris disk from inspecting Sloan Digital Sky Survey (SDSS) spectra of WDs. Possible double-peaked emission lines arising from a gaseous disk are seen in the source’s spectrum. The spectral and imaging data used in our analysis are summarized in Section 2. In Section 3, the analysis and results are presented. We discuss our results in Section 4.

2. DATA

2.1. SDSS Spectra

The source SDSS J114404.74+052951.6 (hereafter SDSS J1144+0529) was first identified by Kepler et al. (2015) as a DA WD using the SDSS spectrum from the SDSS data release (DR) 10. The spectrum was obtained on 2011 April 26 with a signal-to-noise ratio (S/N) of 24 (S/N = 9 in the z' band). On 2012 January 29, the source was observed again by SDSS, and the obtained spectrum led to our serendipitous discovery of the possible presence of a gaseous disk around it (see Figure 1). This spectrum was released in the latest SDSS DR12 with S/N = 29 (16 in the z' band).

2.2. Photometry Data

Optical photometry data $u'g'r'i'z'$ were obtained from the SDSS DR9 (Ahn et al. 2012), while the near-infrared (near-IR) photometry data were obtained from the UKIDSS in the JHK bands taken in 2008 (Lawrence et al. 2007, 2012). There are two imaging observations from UKIDSS in a ~ 3 minute separation. The magnitudes from the two observations are consistent with each other, although because the source is faint, the H and K measurements are within 2σ . The averaged JHK magnitudes were used in the following analysis. A J -band image of the target field is displayed in the left panel of Figure 2. The FWHM of this target’s point-spread function is about $1''.0$. The image clearly shows that there are no other sources close to the WD. A K -band image of the field is displayed in the middle panel of Figure 2. Using the image, we estimated the source counts in the field. Only six sources fainter than SDSS J1144+0529 were detected in a $2' \times 2'$ region around the WD. Given the $1''.0$ FWHM of the source, the possible contamination from faint background sources, i.e., our target containing another source, is extremely low, only 0.03%. The flux measurements for the WD are given in Table 1.

The *WISE* infrared (IR) imaging (Cutri et al. 2013) also detected a source at band *W1* at a position of $0''.7$ away from

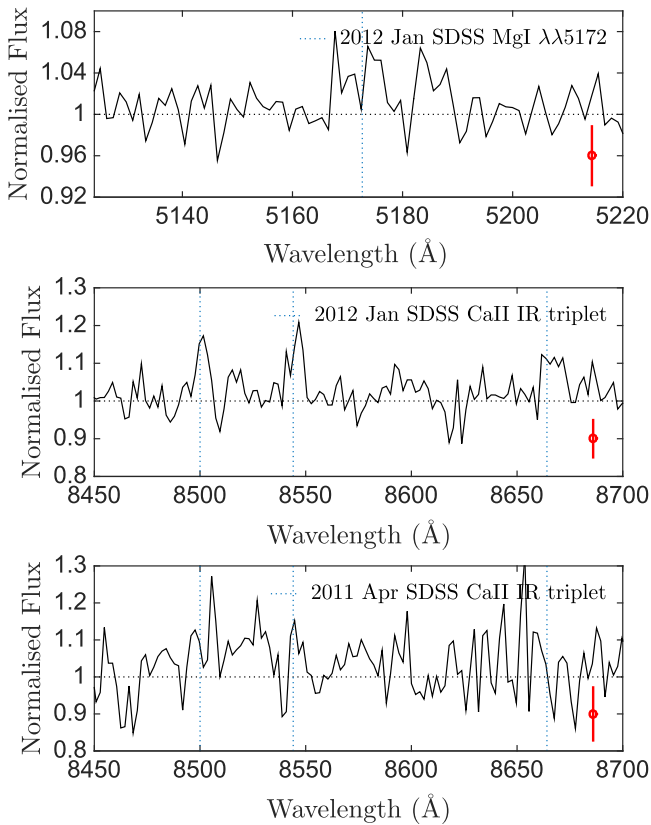


Figure 1. Flux normalized spectra of SDSS J1144+0529. Top and middle panels are the spectrum taken on 2012 January 29, of which the Mg I $\lambda\lambda 5172$ and Ca II IR triplet regions are shown, respectively. Bottom panel shows the spectrum (taken on 2011 April 26) containing the region of the Ca II IR triplet lines. Red circles and bars are typical errors of the relative regions.

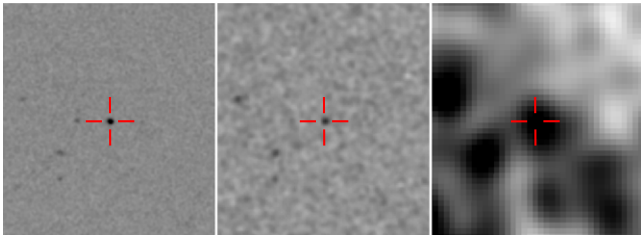


Figure 2. UKIDSS *J* band (left panel), *K* band (middle panel), and WISE *W1* band (right panel) of the SDSS J1144+0529 field. Red crosses are centered at SDSS J1144+0529 with the length of each cross line being $4''$.

that of the WD (see Figure 2). Given the $6''.1$ FWHM for WISE *W1* imaging, the source is consistent with being the counterpart due to the positional coincidence (see, e.g., Debes et al. 2011). The *W1* measurements and *W2*–*W4* flux upper limits are provided in Table 1.

3. ANALYSIS AND RESULTS

3.1. White Dwarf Parameters

We re-analyzed the source with the SDSS 2012 spectrum, which has a higher S/N. The WD atmosphere model provided by Koester (2010) was used. After spectral normalization, Balmer line profiles from H_β to H_ϵ were taken for fitting to the model templates. Detailed fitting processes can be found in Zhao et al. (2013 and references therein). From the fitting, we determined that the effective temperature T_{eff} and surface

gravity g of the WD are $T_{\text{eff}} = 23027 \pm 219$ K and $\log g = 7.74 \pm 0.03$, respectively.

Based on Bergeron’s cooling sequences⁴, the mass and cooling age of this DA WD can be estimated from its T_{eff} and $\log g$. We thus found that the mass is $0.49 \pm 0.03 M_\odot$ and the cooling age is 21.2 ± 1.9 Myr (which is very young for WD cooling ages). Using the SDSS $u'g'r'i'z'$ photometry, estimated T_{eff} , $\log g$, and extinction by adopting the synthetic spectral distance (SSD) estimation method for the DA WD (Holberg et al. 2008), the photometric distance is estimated to be 284.9 ± 13.2 pc. The radius of the WD (R_{WD}) is estimated as $\sim 0.016 R_\odot$. These parameters are consistent with those derived from Kepler et al. (2015).

3.2. IR Excesses

Combining GALEX FUV/NUV, SDSS $u'g'r'i'z'$, UKIDSS *JHK*, and WISE *W1* flux data listed in Table 1, the broadband spectrum for SDSS J1144+0529 was constructed and is shown in Figure 3. Because the source is faint, having a *W1* magnitude larger than 15 mag, an additional 0.2 mag uncertainty was added to the *W1* uncertainty when fitting the model, which accounts for the faintward bias of WISE measurements.⁵ Based on the obtained T_{eff} and $\log g$, the WD model spectrum in the UV, optical, and IR bands is also plotted in the figure. Excess emissions of $\sim 2\sigma$ at the *K* band and $\sim 3\sigma$ at the WISE *W1* band are detected, indicating the possible existence of a dust disk.

A flat, opaque disk model described in Jura (2003) was used to fit the excesses from *J* to *W1*, while the *W2* flux upper limit was included to provide an additional constraint. Based on the fact that this source has IR excesses starting from the near-IR band, which is similar to those of the WD gaseous disk cases (e.g., SDSS 1228+1040, Brinkworth et al. 2009; SDSS 0956–017, Farihi et al. 2012; SDSS 0738+1835 and SDSS 0845+2257, Brinkworth et al. 2012), we fixed the inner disk temperature T_{in} at 1800 K (corresponding to the inner disk radius $r_i \simeq 18 R_{\text{WD}}$). The outer disk radius r_o and inclination angle i were set as free parameters. Within the error range, the distance of 275 pc was adopted here since it provided a better fit, which is similar to the case of SDSS J0738+1835 from Brinkworth et al. (2012). The best fit was obtained when $r_o \simeq 53 R_{\text{WD}}$ (corresponding to ~ 800 K for outer disk temperature), $i = 82^\circ$, and the minimum $\chi^2 = 3.9$ (for 2 degrees of freedom (dof)). The disk model fit is overplotted as a dashed–dotted curve in Figure 3. For the inner disk temperature fixed at 1400 K (corresponding to the inner disk radius $r_i \simeq 25 R_{\text{WD}}$), the best fit was found to be $r_o \simeq 74 R_{\text{WD}}$ (corresponding to ~ 600 K for outer disk temperature), $i = 82^\circ$, and the minimum $\chi^2 = 8.1$ (2 dof). According to the fitting results in Figure 3, the faintward bias as much as ~ 0.2 mag could be real. Therefore, a more accurate, brighter *W1* measurement, which accounts for the faintward bias, can improve the fit a lot.

Although it is unlikely to have a low-mass companion for the WD, since no stellar features are seen in the IR region of the SDSS spectra, we tested to fit the excesses with a blackbody. We found a temperature of 2900 K and $0.07 R_\odot$ can provide the best fit ($\chi^2 = 2.2$ for 3 dof). The mid-type M dwarfs can match the temperature, but they are too large to fit in the small radius size (e.g., Kaltenegger & Traub 2009).⁶ In other words,

⁴ <http://www.astro.umontreal.ca/~bergeron/CoolingModels/>

⁵ See http://wise2.ipac.caltech.edu/docs/release/allwise/expsup/sec2_2.html

⁶ See also <http://www.johnstonsarchive.net/astro/browndwarflist.html>

Table 1
Broadband Photometry of SDSS J1144+0529

GALEX—Ultraviolet					
Band	FUV	NUV			
Wavelength (nm)	152.9	231.2			
m (mag)	16.495 ± 0.032	16.861 ± 0.025			
Flux _{obs} (mJy)	0.912 ± 0.025	0.665 ± 0.018			
SDSS—Optical					
Band	u'	g'	r'	i'	z'
Wavelength (nm)	355.1	468.6	616.5	748.1	893.1
m (mag)	17.270 ± 0.009	17.292 ± 0.005	17.697 ± 0.006	17.951 ± 0.009	18.263 ± 0.033
Flux (mJy)	0.490 ± 0.004	0.469 ± 0.002	0.317 ± 0.002	0.248 ± 0.002	0.184 ± 0.006
UKIDSS—IR					
Band	J	H	K		
Wavelength (nm)	1248	1631	2201		
m (mag)	17.793 ± 0.031	17.796 ± 0.106	17.454 ± 0.123		
	17.767 ± 0.028	17.588 ± 0.083	17.810 ± 0.164		
Flux _{average} (mJy)	0.120 ± 0.005	0.086 ± 0.011	0.056 ± 0.012		
WISE—Infrared					
Band	$W1$	$W2$	$W3$	$W4$	
Wavelength (μ m)	3.4	4.6	12	22	
m (mag)	17.31 ± 0.16	16.54	11.91	8.49	
Flux (mJy)	0.037 ± 0.006	0.04	0.50	3.34	

significant excess fluxes would be detected at the z' and J bands.

3.3. Gas Emission Lines

As shown in the top and middle panels of Figure 1, the Ca II IR triplet emission lines were weakly detected in the SDSS 2012 spectrum with equivalent widths (EWs) of $-1.3 \pm 0.4 \text{ \AA}$, $-1.7 \pm 0.4 \text{ \AA}$, and $-1.5 \pm 0.5 \text{ \AA}$, respectively. There is also a possible detection of Mg I $\lambda\lambda 5172$ with an EW of $-0.6 \pm 0.4 \text{ \AA}$. The Ca II IR triplet lines show mildly double-peaked morphology and are quite similar to that seen in HE 1349–2305 (Melis et al. 2012a). The 2011 spectrum, shown in the bottom panel of Figure 1, is too noisy to be determined, whether or not the lines are present. The upper limits (1σ) on their EWs are $<-1.6 \text{ \AA}$, $<-0.7 \text{ \AA}$, and $<-0.3 \text{ \AA}$ for the Ca II IR triplet. We also went through the spectra for absorption lines of heavy elements (e.g., Melis et al. 2012a), which would indicate a polluted atmosphere due to accretion from the disk, but only the weak Ca II K line in the 2012 SDSS spectrum is marginally detected. Therefore, nearly no evident heavy element absorption lines were detected in the available spectra, which is most likely due to the spectra quality not being good enough.

The double-peaked line profiles can be used to constrain the physical size of the gaseous disk (Gänsicke et al. 2006). However, given the weak detection of the lines in our case, we only estimated the values for the maximum Doppler-shifted velocities v_{\max} of the Ca II IR triple emission lines in the 2012 SDSS spectrum. We found $v_{\max} \sin i = -354 \pm 141/211 \pm 106 \text{ km s}^{-1}$, $v_{\max} \sin i = -179 \pm 70/313 \pm 140 \text{ km s}^{-1}$, and $v_{\max} \sin i = -143 \pm 69/411 \pm 138 \text{ km s}^{-1}$ (see Horne & Marsh 1986; Gänsicke et al. 2006). Considering $i \sim 82^\circ$ from the dust disk fitting, the estimations imply that the inner radii of

the gas disk are $\sim 30 R_{\text{WD}}$. While the uncertainties are large, the value is in agreement with those of previously reported gaseous disks (e.g., Gänsicke et al. 2008; Melis et al. 2012a; Wilson et al. 2014).

4. DISCUSSION

We have serendipitously discovered a highly likely debris disk around the recently identified DA WD SDSS J1144+0529. The Ca II IR triplet and possible Mg I $\lambda\lambda 5172$ emission lines, although are weak, show a double-peaked profile, which is the hallmark for the presence of a gaseous disk (Gänsicke et al. 2006). Further analyzing the IR archival data, significant excess emission above the thermal surface emission from the WD has also been found. Such IR excesses are expected for WD debris-disk systems since, so far, all the identified gaseous disks have been found to also contain a significant amount of dust by showing excess IR emission (Brinkworth et al. 2009, 2012). Further confirmation and follow-up studies of the debris disk around SDSS J1144+0529 can be easily conducted through optical spectroscopy and IR imaging with a large telescope.

In the study of the IR excesses in four WD gaseous disks, Brinkworth et al. (2012) noted that T_{in} higher than the 1400 K (sublimation temperature) is favored when the commonly used debris-disk model, proposed by Jura (2003), is used to fit the excesses. This is also true in our case. It is possible that the debris-disk model is too simplified, or as suggested by Rafikov & Garmilla (2012), the inner part of a debris disk could have a much higher sublimation temperature because of the high metal vapor pressure. For the latter possibility in particular, the gaseous debris disks might indeed be the observational samples.

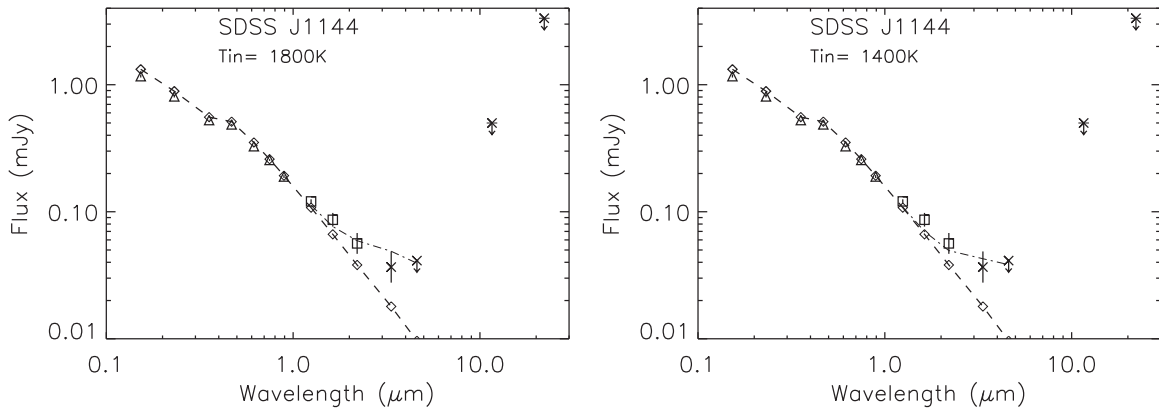


Figure 3. Flux density spectra of SDSS J1144+0529. The UV *GALEX* FUV/NUV, optical SDSS $u'g'r'i'z'$, UKIDSS *JHK*, and *WISE* *W1–W4* fluxes and flux upper limits are marked as triangles, triangles, squares, and crosses, respectively. The WD model fluxes are shown as diamonds and connected by the dashed curve. The debris-disk model fit to the IR excesses is plotted as a dashed-dotted curve, where the left panel shows the case of $T_{\text{in}} = 1800$ K and the right panel the case of $T_{\text{in}} = 1400$ K.

In any case, the properties of $\sim 23,000$ K temperature and a cooling age of ~ 21 Myr make SDSS J1144+0529 one of the hottest and youngest WDs with a debris disk (Hoard et al. 2013; Rocchetto et al. 2015). The properties are also in line with the likely conditions for WDs to have a sufficiently bright debris disk as well (Gänsicke et al. 2006, 2008; Dufour et al. 2012; Farihi et al. 2012). The WD should also be polluted due to accretion from the disk, and thus absorption features of heavy elements in its optical spectra are expected. These features are normally very weak, which is probably the reason that only Ca II *K* is seen in the SDSS 2012 spectrum that we have analyzed. Deep spectroscopic observations with a large telescope will confirm the presence of heavy elements in the atmosphere of this WD.

We thank the anonymous referee for helpful suggestions that have improved the paper greatly. We thank D. Koester and P. Bergeron for providing WD models. Balmer/Lyman lines in the models were calculated with the modified Stark broadening profiles of Tremblay & Bergeron (2009), kindly made available by the authors. The authors acknowledge the National Science Foundation of China (NSFC) under grants NSFC-11333004, U1431106. A.T. acknowledges support from Chinese Academy of Sciences visiting Fellowship for Researchers from Developing Countries.

REFERENCES

- Ahn, C. P., Alexandroff, R., Allende Prieto, C., et al. 2012, *ApJS*, **203**, 21
- Brinkworth, C. S., Gänsicke, B. T., Girven, J. M., et al. 2012, *ApJ*, **750**, 86
- Brinkworth, C. S., Gänsicke, B. T., Marsh, T. R., Hoard, D. W., & Tappert, C. 2009, *ApJ*, **696**, 1402
- Cutri, R. M., Wright, E. L., Conrow, T., et al. 2013, *yCat*, **2328**, 0
- Debes, J. H., Hoard, D. W., Wachter, S., Leisawitz, D. T., & Cohen, M. 2011, *ApJS*, **197**, 38
- Debes, J. H., & Sigurdsson, S. 2002, *ApJ*, **572**, 556
- Dufour, P., Kilic, M., Fontaine, G., et al. 2012, *ApJ*, **749**, 6
- Farihi, J., Gänsicke, B. T., & Koester, D. 2013, *Sci*, **342**, 218
- Farihi, J., Gänsicke, B. T., Steele, P. R., et al. 2012, *MNRAS*, **421**, 1635
- Gänsicke, B. T., Koester, D., Marsh, T. R., Rebassa-Mansergas, A., & Southworth, J. 2008, *MNRAS*, **391**, L103
- Gänsicke, B. T., Marsh, T. R., & Southworth, J. 2007, *MNRAS*, **380**, L35
- Gänsicke, B. T., Marsh, T. R., Southworth, J., & Rebassa-Mansergas, A. 2006, *Sci*, **314**, 1908
- Graham, J. R., Matthews, K., Neugebauer, G., & Soifer, B. T. 1990, *ApJ*, **357**, 216
- Hoard, D. W., Debes, J. H., Wachter, S., Leisawitz, D. T., & Cohen, M. 2013, *ApJ*, **770**, 21
- Holberg, J. B., Bergeron, P., & Gianninas, A. 2008, *AJ*, **135**, 1239
- Horne, K., & Marsh, T. R. 1986, *MNRAS*, **218**, 761
- Jura, M. 2003, *ApJL*, **584**, L91
- Jura, M. 2008, *AJ*, **135**, 1785
- Kaltenegger, L., & Traub, W. A. 2009, *ApJ*, **698**, 519
- Kepler, S. O., Pelisoli, I., Koester, D., et al. 2015, *MNRAS*, **446**, 4078
- Klein, B., Jura, M., Koester, D., & Zuckerman, B. 2011, *ApJ*, **741**, 64
- Koester, D. 2010, *MmSAI*, **81**, 921
- Lawrence, A., Warren, S. J., Almaini, O., et al. 2007, *MNRAS*, **379**, 1599
- Lawrence, A., Warren, S. J., Almaini, O., et al. 2012, *yCat*, **2314**, 0
- Melis, C., Dufour, P., Farihi, J., et al. 2012, *ApJL*, **751**, L4
- Raddi, R., Gänsicke, B. T., Koester, D., et al. 2015, *MNRAS*, **450**, 2083
- Rafikov, R. R., & Garmilla, J. A. 2012, *ApJ*, **760**, 123
- Rocchetto, M., Farihi, J., Gänsicke, B. T., & Bergfors, C. 2015, *MNRAS*, **449**, 574
- Tremblay, P.-E., & Bergeron, P. 2009, *ApJ*, **696**, 1755
- Veras, D., Mustill, A. J., Bonsor, A., & Wyatt, M. C. 2013, *MNRAS*, **431**, 1686
- Wilson, D. J., Gänsicke, B. T., Koester, D., et al. 2014, *MNRAS*, **445**, 1878
- Xu, S., Jura, M., Koester, D., Klein, B., & Zuckerman, B. 2014, *ApJ*, **783**, 79
- Zhao, J. K., Luo, A. L., Oswalt, T. D., & Zhao, G. 2013, *AJ*, **145**, 169
- Zuckerman, B., & Becklin, E. E. 1987, *Natur*, **330**, 138
- Zuckerman, B., Koester, D., Melis, C., Hansen, B. M., & Jura, M. 2007, *ApJ*, **671**, 872
- Zuckerman, B., Koester, D., Reid, I. N., & Hünsch, M. 2003, *ApJ*, **596**, 477